

# Synchronization of rigid microrotors by time-dependent hydrodynamic interactions

Mario Theers\* and Roland G. Winkler†

*Theoretical Soft Matter and Biophysics, Institute for Advanced Simulation and Institute of Complex Systems,  
Forschungszentrum Jülich, D-52425 Jülich, Germany*

(Received 22 April 2013; published 13 August 2013)

We investigate the emergent dynamical behavior of hydrodynamically coupled microrotors. The two rotors are confined in a plane and move along circles driven by active forces. The three-dimensional fluid is described by the linearized, time-dependent Navier-Stokes equations instead of the usually adopted Stokes equations. We demonstrate that time-dependent hydrodynamic interactions lead to synchronization of the rotational motion. The time dependence of the phase difference between the rotors is determined and synchronization times are extracted for various external torques and rotor separations by solving the underlying integrodifferential equations numerically. In addition, an analytical expression is provided for the synchronization time.

DOI: [10.1103/PhysRevE.88.023012](https://doi.org/10.1103/PhysRevE.88.023012)

PACS number(s): 47.63.-b, 05.45.Xt, 87.17.Jj

## I. INTRODUCTION

Synchronization is a common phenomenon in nonlinear systems and consequently is omnipresent in nature and technical applications. The phenomenon appears at all length scales from atoms to macroscopic bodies [1,2]. On the microscale, synchronization is fundamental for the motility of microswimmers which exploit flagella for their propulsion, such as spermatozoa, bacteria, protozoa, or algae [3]. Consequently, various concepts for microscopic synchronization have been developed and suggested. The synchronized beating of nearby swimming spermatozoa was first modeled and analyzed in Ref. [4]. This study suggests that hydrodynamic interactions lead to synchronization, an aspect which has received considerable theoretical [5–15] and experimental [16–21] attention since then. However, synchronization is not easily achieved for low Reynolds-number fluids, which are described by Stokes equations [22]. The presence of kinematic reversibility of the swimmer motion combined with swimmer symmetries may prevent synchronization [5,6,11]. This fundamental limitation can be overcome by implementation of a system flexibility [6,17,23–25] or by specific, nonreversible driving forces [13]. Alternatively, synchronization of beating flagella, e.g., of *Chlamydomonas*, could also be achieved nonhydrodynamically. As discussed in Ref. [26] flagella synchronization follows from hydrodynamic friction forces, which couple the flagellar oscillations via movement of the swimmer (see also Ref. [27]).

Theoretical studies typically adopt the solution of the Stokes equations to describe the hydrodynamic interactions between active objects [5,6,8–11,13–15]. Here, the inertial forces in the Navier-Stokes equations are assumed to be small compared to viscous forces and are therefore neglected. This is certainly justified for the nonlinear advective term [3,22], but it is less evident for the time derivative of the velocity (temporal acceleration), since the latter renders the resulting equations irreversible. Hence, we expect the time derivative of the velocity to affect the dynamical behavior of hydrodynamically coupled active objects with corresponding

irreversible dynamics, which may lead to their synchronized motion. A strong influence of the temporal acceleration term on the fluid structure has been demonstrated for other fluid systems, e.g., in Ref. [28] it has been shown that reversibly and periodically driven systems can respond with an irreversible flow field.

In this article, we study the emergent dynamical properties of two hydrodynamically coupled circular rotors. Rigid-body rotors are model systems to study hydrodynamic interactions and synchronization between flagella or cilia [8,9,13]. Due to their high symmetry and reversible dynamics, such rotors belong to the general class of systems, where additional measures have to be taken to achieve synchronization, despite strong hydrodynamic interactions, provided that they are described by Stokes equations [6,13,17,23]. As an extension, we take into account the time dependence of the hydrodynamic interactions. We demonstrate that the presence of the temporal acceleration term leads to synchronization of the rotor dynamics. Hence, our studies provide a counterexample to the paradigm that highly symmetric systems at low Reynolds number require additional measures to achieve a synchronized motion.

## II. MODEL

We adopt the rotor model of Ref. [8]: Two beads of radius  $a$  move along circles of radius  $R$ , each driven by an active force  $\mathbf{F}_i$  (cf. Fig. 1). The two circles are centered at  $\mathbf{r}_i^0 = (-1)^i(d/2)\mathbf{e}_x$  ( $i = 1,2$ ), where  $\mathbf{e}_x$  is the unit vector along the  $x$  axis and  $d$  the center-to-center distance, and both beads are confined in the  $xy$  plane. The trajectories of the bead centers can be expressed as

$$\mathbf{r}_i(t) = \mathbf{r}_i^0 + [R \cos \varphi_i(t), R \sin \varphi_i(t), 0]^T, \quad (1)$$

in terms of the phase angles  $\varphi_i(t)$ . The driving forces

$$\mathbf{F}_i(t) = F \mathbf{t}_i(t) \quad (2)$$

are of equal magnitude and point along the tangents  $\mathbf{t}_i(t)$  of the trajectories, where

$$\mathbf{t}_i(t) = [-\sin \varphi_i(t), \cos \varphi_i(t), 0]^T. \quad (3)$$

\*m.theers@fz-juelich.de

†r.winkler@fz-juelich.de

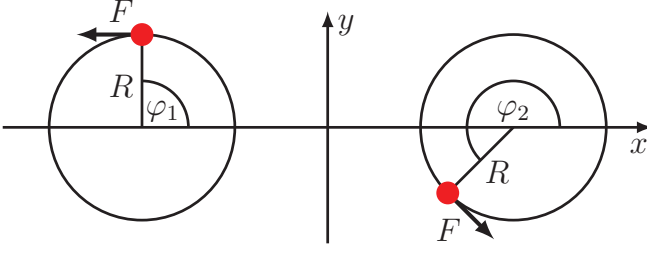


FIG. 1. (Color online) Model system [8]: Two beads move along fixed circular trajectories, each driven by a constant tangential force  $F$ .

The beads are immersed in an incompressible fluid, which is described by the linearized Navier-Stokes equations

$$\rho \frac{\partial \mathbf{v}}{\partial t} = -\nabla p + \eta \Delta \mathbf{v} + \mathbf{f}, \quad \nabla \cdot \mathbf{v} = 0, \quad (4)$$

i.e., we neglect the convective acceleration term.  $\mathbf{v}(\mathbf{r}, t)$  is the fluid velocity field at the point  $\mathbf{r}$  in space and time  $t$ ,  $\rho$  its density,  $p(\mathbf{r}, t)$  is the pressure,  $\eta$  the viscosity, and  $\mathbf{f}(\mathbf{r}, t)$  a volume force acting on the fluid. Taking as characteristic values  $d \approx R \approx 1 \mu\text{m}$  and the rotation frequency  $\omega \approx 100/\text{s}$ , corresponding to micrometer size swimmers [3,19,29], the Reynolds number becomes  $\text{Re} \approx 10^{-4}$  in water. Hence, the convective acceleration term can well be neglected compared to the viscous term. We retain the term  $\rho \partial \mathbf{v} / \partial t$ , because we are interested in effects due to the broken time reversibility of Eq. (4).

The solution of the linear equations (4) can be expressed in terms of the hydrodynamic tensor  $\mathbf{Q}(\mathbf{r}, t)$  as [30–32]

$$\mathbf{v}(\mathbf{r}, t) = \int_{\mathbb{R}^3} d^3 r' \int_0^t dt' \mathbf{Q}(\mathbf{r} - \mathbf{r}', t - t') \mathbf{f}(\mathbf{r}', t'), \quad (5)$$

with the Cartesian components

$$Q_{\alpha\beta}(\mathbf{r}, t) = \frac{1}{\rho} \left[ A(r, t) \delta_{\alpha\beta} - B(r, t) \frac{r_\alpha r_\beta}{r^2} \right], \quad (6)$$

$\alpha, \beta \in \{x, y, z\}$ ,  $r = |\mathbf{r}|$ , and [30]

$$\begin{aligned} A(r, t) &= \left( 1 + \frac{2vt}{r^2} \right) f(r, t) - \frac{g(r, t)}{r^2}, \\ B(r, t) &= \left( 1 + \frac{6vt}{r^2} \right) f(r, t) - \frac{3g(r, t)}{r^2}, \\ f(r, t) &= \frac{1}{(4\pi vt)^{3/2}} \exp\left(-\frac{r^2}{4vt}\right), \\ g(r, t) &= \frac{1}{4\pi r} \text{erf}\left(\frac{r}{\sqrt{4vt}}\right). \end{aligned} \quad (7)$$

Imposing no-slip boundary conditions on the surfaces  $S_i$  of the solid spherical beads, the equations of motion of the rotors are [22]

$$\dot{\mathbf{r}}_i = \frac{1}{4\pi a^2} \oint_{S_i} d^2 r \mathbf{v}(\mathbf{r}, t). \quad (8)$$

In the limit of  $a/R \ll 1$ , i.e., pointlike particles, the integration over a bead surface can be performed and Eqs. (8)

yield

$$\dot{\mathbf{r}}_i(t) = \frac{1}{\gamma} \mathbf{F}_i(t) + \sum_{j \neq i} \int_0^t dt' \mathbf{Q}(\mathbf{r}_i(t) - \mathbf{r}_j(t'), t - t') \mathbf{F}_j(t'). \quad (9)$$

Here, we assume that the drag force  $\mathbf{F}_i^h$  on a particle is balanced by the driving force  $\mathbf{F}_i$ , which implies  $\mathbf{F}_i^h + \mathbf{F}_i = \mathbf{0}$ , i.e., bead inertia is neglected. The first term on the right hand side of Eq. (9) corresponds to Stokes law, with the friction coefficient  $\gamma = 6\pi\eta a$ ; it describes the local frictional properties of a bead. The second term accounts for interbead hydrodynamic interactions.

The creeping flow limit follows by assuming that  $\mathbf{r}_j(t)$ , and hence  $\mathbf{F}_j(t)$ , changes significantly slower than  $\mathbf{Q}(\mathbf{r}, t)$  with time. With constant  $\mathbf{r}_j$  and  $\mathbf{F}_j$ , integration of  $\mathbf{Q}(\mathbf{r}, t)$  over time yields, in the asymptotic limit of large  $t$ , the well-known Oseen tensor and, in addition, a time-dependent correction term which is proportional to  $1/\sqrt{t}$ . Hence, the asymptotic limit is reached only very slowly, which indicates a strong influence of time-dependent hydrodynamic correlations on the bead motion.

Using the position vectors (1) and forces (2), Eqs. (9) yield the coupled integrodifferential equations

$$\dot{\varphi}_i = \omega + \frac{F}{R} \sum_{j \neq i} \int_0^t dt' \mathbf{t}_i(t) \cdot \mathbf{Q}(\mathbf{r}_i(t) - \mathbf{r}_j(t'), t - t') \mathbf{t}_j(t') \quad (10)$$

for the phase angles, with the intrinsic angular frequency  $\omega = F/(\gamma R) = 2\pi/T$  and  $T$  the rotation period. In the creeping-flow limit, i.e., by neglecting all time-dependent correlations, this equation turns into the equation considered in Refs. [8,13], and synchronization of the bead rotation is not possible.

The coupled equations (10) can only be solved numerically and with considerable effort due to the nonlinear coupling. Therefore, we apply the mean-field approximation  $\mathbf{r}_2(t) - \mathbf{r}_1(t') \approx d\mathbf{e}_x$ , which strictly applies for  $d/R \gg 1$ . Tests confirm that the dynamical behavior is well described by this approximation for the parameters considered in the following. Then, Eqs. (10) turn into

$$\frac{d\varphi_i}{d\tau} = 2\pi + \frac{3\Lambda}{2} \int_0^\tau d\tau' \mathbf{t}_i(\tau) \cdot \mathbf{Q}(\chi, \tau - \tau') \mathbf{t}_j(\tau'), \quad (11)$$

when we introduce the dimensionless time  $\tau = t/T$  and the abbreviation  $\Lambda = 8\pi^2 a/(d\chi)$ , where  $\chi = d^2/(vT)$  is the ratio of the viscous time scale  $d^2/v$  and the rotation period  $T$ . The tensor  $\mathbf{Q}(\chi, \tau)$  follows from Eq. (6) and reads as

$$Q_{\alpha\beta}(\chi, \tau) = A(\chi, \tau) \delta_{\alpha\beta} - B(\chi, \tau) \delta_{\alpha x} \delta_{\beta x}, \quad (12)$$

with  $A(\chi, \tau) = d^3 A(d, t)$  and  $B(\chi, \tau) = d^3 B(d, t)$ .

### III. SYNCHRONIZATION: NUMERICAL AND ANALYTICAL SOLUTIONS

#### A. Numerical solution for phases

The numerical solutions of Eqs. (10) and (11) are obtained by a combination of Euler's integration scheme and the trapezoidal rule [33]. The time dependence of the deviatoric phases  $\Delta\varphi_i = \varphi_i - 2\pi\tau$  is depicted in Fig. 2. The initial phase difference  $\pi/2$  clearly vanishes in the asymptotic limit of large

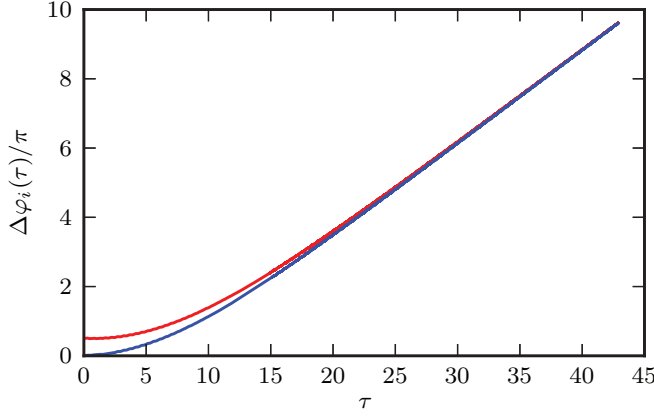


FIG. 2. (Color online) Deviatoric phases  $\Delta\varphi_i(\tau) = \varphi_i - 2\pi\tau$  for the parameters  $\Lambda = 10^4$  and  $\chi = 10^{-3}$ , and the initial phase difference  $\pi/2$ .

times. Hence, hydrodynamic correlations lead to synchronization of the rotational motion. Interestingly, the deviatoric phases increase with increasing time. Hence, hydrodynamic interactions lead to a faster increase of the  $\varphi_i$  than Stokes friction alone. As an example, the time derivative of  $\Delta\varphi_1$  is shown in Fig. 3. It clearly increases with time due to hydrodynamic interactions. Such an increase is already predicted by the solution of the rotor equations based on Stokes equation [13,14,34], where the average angular velocity can be easily computed as

$$\langle \dot{\varphi}_i \rangle = \left\langle \frac{F}{\gamma R} \left[ 1 + \frac{6a}{8d} (1 + \sin^2(\varphi_i)) \right] \right\rangle = \frac{F}{\gamma R} \left[ 1 + \frac{9a}{8d} \right]. \quad (13)$$

This corresponds to a relative increase of  $\Delta\dot{\varphi}_i = 9a/8d$  in angular velocity. However, hydrodynamic correlations yield a somewhat lower asymptotic value. By fast Fourier transformation (FFT), we obtain an average value for  $\Delta\dot{\varphi}_i$ , which is approximately 6% smaller for the parameters of Fig. 3. Qualitatively, the high frequency oscillations of  $\Delta\dot{\varphi}_1$  (Fig. 3) can be traced back to the sine-square term in Eq. (13). However, for Eq. (11), the actual term is somewhat more complicated [cf. Eq. (14)].

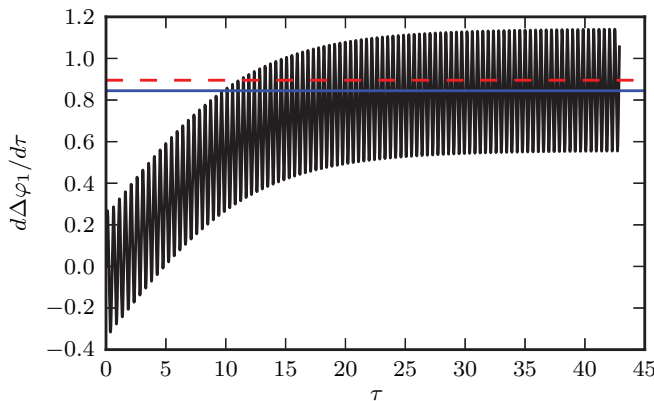


FIG. 3. (Color online) Frequency of the deviatoric phase  $\Delta\varphi_1$  for  $\Lambda = 10^4$  and  $\chi = 10^{-3}$ . The blue solid line is the asymptotic average frequency. The red dashed line represents the result of Eq. (13), which is about 6% larger.

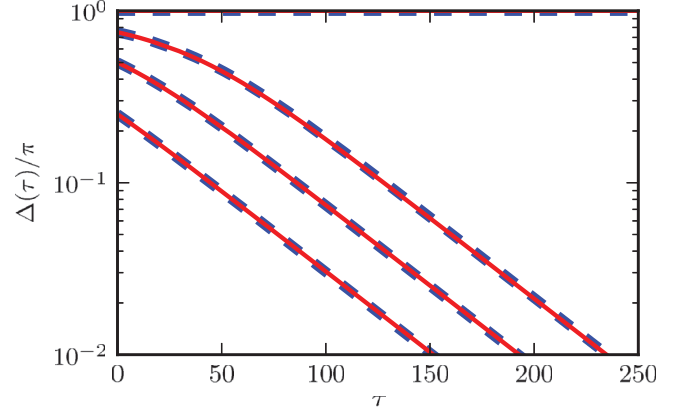


FIG. 4. (Color online) Phase differences  $\Delta(\tau) = \varphi_1(\tau) - \varphi_2(\tau)$  for the initial conditions  $\Delta(0) = \pi, 3\pi/4, \pi/2,$  and  $\pi/4$  (top to bottom),  $\chi = 6.25 \times 10^{-6}$ ,  $\Lambda = 5 \times 10^3$ , and  $d/R = 2.5$ . The dashed lines are numerical solutions of Eqs. (10) and the solid lines are the solutions of Eqs. (11). Note that  $\Delta(0) = \pi$  is an unstable fixed point.

Figure 4 presents numerical solutions for the phase differences  $\Delta(\tau) = \varphi_1(\tau) - \varphi_2(\tau)$  of both Eqs. (10) and the mean-field anisotropic equations (11). The two solutions agree very well and are hardly distinguishable in the representation of Fig. 4. As is already evident from Fig. 2, the phase difference vanishes for long times and the rotors exhibit a synchronized rotational motion with zero phase difference.

## B. Analytical approximation

In order to characterize the asymptotic exponential decay of the phase difference (cf. Fig. 4), we derive an approximate analytical solution of Eq. (11). With the tangent vectors (3), Eqs. (11) become

$$\frac{d\varphi_i}{d\tau} = 2\pi + \frac{3\Lambda}{2} \sum_{j \neq i} \int_0^\tau d\tau' \left[ \left( A - \frac{B}{2} \right) \cos[\varphi_i(\tau) - \varphi_j(\tau')] \right] + \frac{B}{2} \cos[\varphi_i(\tau) + \varphi_j(\tau')], \quad (14)$$

where  $A = A(\chi, \tau - \tau')$  and  $B = B(\chi, \tau - \tau')$ . The nonlinear coupling between the phases  $\varphi_i$  via the cosine is reminiscent of the sine coupling in the Kuramoto model [35,36]. However, in our model the interaction is retarded;  $\varphi_i(\tau)$  couples to  $\varphi_j(\tau')$  for  $0 < \tau' < \tau$  and vice versa.

Using trigonometric identities and the definition  $\sigma(\tau) = \Delta\varphi_1(\tau) + \Delta\varphi_2(\tau)$ , we obtain the equation of motion for the phase difference

$$\begin{aligned} \frac{d\Delta}{d\tau} = & -3\Lambda \int_0^\tau d\tau' \left[ A - \frac{B}{2} \right] \sin \left( \frac{\Delta(\tau) + \Delta(\tau')}{2} \right) \\ & \times \sin \left( 2\pi(\tau - \tau') + \frac{\sigma(\tau) - \sigma(\tau')}{2} \right) \\ & - 3\Lambda \int_0^\tau d\tau' \frac{B}{2} \sin \left( \frac{\Delta(\tau) - \Delta(\tau')}{2} \right) \\ & \times \sin \left( 2\pi(\tau + \tau') + \frac{\sigma(\tau) + \sigma(\tau')}{2} \right). \end{aligned} \quad (15)$$

Here, we already see that  $\Delta(\tau) = 0$ ,  $\tau \geq 0$ , is a solution of the equation, and hence a fixed point. To derive an analytical solution, we will apply the following approximations. (i) The hydrodynamic functions  $A(\chi, \tau)$  and  $B(\chi, \tau)$  are peaked at  $\tau \approx \chi \ll 1$ , hence, we set  $\Delta(\tau') \approx \Delta(\tau)$  and  $\sigma(\tau') \approx \sigma(\tau)$ . Note that a similar approximation is applied in the creeping-flow approximation of Eq. (5), when  $f(\mathbf{r}', t')$  is replaced by  $f(\mathbf{r}', t)$ , which leads to the Stokes solution after time integration from 0 to  $\infty$ . Here, we only replace  $\tau'$  by  $\tau$  for the slowly varying functions  $\sigma$  and  $\Delta$ , but not for  $\sin[2\pi(\tau - \tau')]$ . (ii) We consider the case  $0 < \Delta(0) \ll 1$  and assume that  $\Delta(\tau)$  will stay small, which allows us to linearize the equations of motion in  $\Delta(\tau)$ . (iii) We approximate  $A - B/2$  by its leading order term for  $\chi/\tau \ll 1$ , which is justified, since we are interested in the time range  $\tau \gg \chi$ . This leads to the separable linear differential equation

$$\frac{d}{d\tau} \Delta(\tau) = -2\Lambda \int_0^\tau d\tau' \left( \frac{\chi}{4\pi\tau} \right)^{3/2} \sin(2\pi\tau') \Delta(\tau). \quad (16)$$

Interestingly, Eq. (16) is also obtained, when the anisotropic tensor  $\mathbf{Q}(r, t)$  in Eq. (10) is replaced by its isotropic average  $\langle Q_{\alpha\beta} \rangle = 2f(r, t)/(3\rho)\delta_{\alpha\beta}$  and the same approximations are applied.

The solution of Eq. (16) is

$$\Delta(\tau) = \Delta(0) \exp\left(-\int_0^\tau \tau_s(\tau')^{-1} d\tau'\right), \quad (17)$$

with the abbreviation

$$\tau_s(\tau) = \left[ 2\Lambda \int_0^\tau d\tau' \left( \frac{\chi}{4\pi\tau} \right)^{3/2} \sin(2\pi\tau') \right]^{-1}. \quad (18)$$

In the long-time limit  $\tau \rightarrow \infty$ , the integral in Eq. (18) can be evaluated and the phase difference exhibits the exponential decay  $\exp(-\tau/\tau_s)$  with the synchronization time

$$\tau_s = \frac{\sqrt{4\pi}}{\Lambda\chi^{3/2}} = \frac{\sqrt{\nu T/a^2}}{4\pi^{3/2}}. \quad (19)$$

Evidently, the differences  $\Delta(\tau)$  decay with increasing time  $\tau$  for all initial values  $\Delta(0)$ , except for  $\Delta(0) = \pi$  (cf. Fig. 4). Similar to the derivation of Eqs. (15) and (16), it can be shown that  $\Delta(0) = \pi$  corresponds to an unstable fixed point; without perturbation, the rotors are phase locked and move synchronously. Moreover, our numerical calculations consistently confirm that  $\Delta(0) = 0$  is a stable fixed point. Above an initial-condition-dependent time  $\tau_0$ ,  $\Delta(\tau)$  decays exponentially, as predicted by the analytical solution (17). Hence, the time-dependent hydrodynamic coupling leads to a synchronized rotation of the two rotors.

### C. Synchronization time

The synchronization time depends on the parameters  $\chi$  and  $\Lambda$ . For an estimation of suitable values for  $\chi$  and  $\Lambda$ , we adopt characteristic values for *E. coli* flagella [37] and the kinematic viscosity of water, i.e., we set  $d/R \approx 2.5$ ,  $d/a \approx 50$ , and  $T \approx 10^{-2}$  s, which yields  $\chi \approx 10^{-4}$  and  $\Lambda \approx 10^4$ . Hence, we consider the ranges  $\chi = 10^{-2}$ – $10^{-4}$  and  $\Lambda = 10^2$ – $10^4$ . In order to extract the synchronization time  $\tau_s$  from the

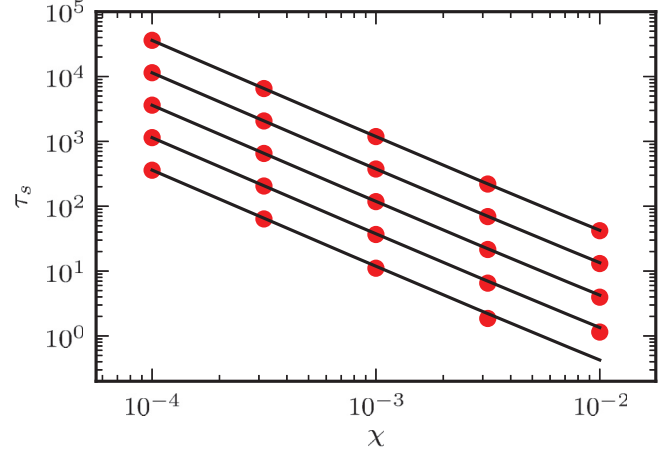


FIG. 5. (Color online) Synchronization times  $\tau_s$  for the parameters  $\Lambda = 10^2, 3.16 \times 10^2, 10^3, 3.16 \times 10^3$ , and  $10^4$  (top to bottom). The bullets are the synchronization times extracted from the numerically obtained  $\Delta(\tau)$  by a fit of an exponential function for  $\tau > \tau_0$  (cf. Fig. 4), where  $\tau_0$  is the time where the exponential decay starts. The solid lines are the theoretically expected values according to Eq. (19).

numerically determined phase differences, we fit  $\Delta(\tau)$  by an exponential function for sufficiently long times  $\tau > \tau_0$ . The corresponding results are presented in Fig. 5. Evidently, the analytical prediction (19) closely follows the numerical values.

A large range of synchronization times is covered by the parameters of Fig. 5. Since  $\tau_s = t_s/T$ , several thousand rotational periods are required to achieve synchronization for small  $\chi$  and  $\Lambda$ . However, by an appropriate choice of these values, synchronization is possible within a few tens of rotations only. Using  $\chi = 4 \times 10^{-3}$ , i.e., the rotation period is very small compared to the viscous time, and  $\Lambda = 300$ , which corresponds to  $a/d = 0.02$ , the synchronization time is  $\tau_s = 50$ .

## IV. SUMMARY

We have used a simple model to demonstrate that time-dependent hydrodynamic interactions alone can lead to a synchronized motion of two rotors. An initial phase difference decays exponentially above a certain time, with a characteristic time, which, in the limit  $\chi \ll 1$ , depends only on the ratio of the rotation period and the viscous time  $a^2/\nu$  for momentum diffusion over the bead radius  $a$ . Thermal fluctuations influence the synchronization behavior of the rotors. Unfortunately, such fluctuations cannot be easily incorporated in an analytical theory, because the description in terms of generalized coordinates leads to multiplicative noise terms. However, we have performed computer simulations employing the multiparticle collision dynamics (MPC) method [38–40], which naturally includes thermal fluctuations. These simulations yield average phase differences which quantitatively agree with those obtained by the solutions of Eqs. (10). Hence, synchronization is stable with respect to thermal fluctuations. This emphasizes the relevance of the time dependence of hydrodynamic interactions

on the emergent dynamical behavior of driven microscopic objects.

In general, various mechanisms lead to flagella synchronization of microswimmers such as *E. coli* or *Chlamydomonas*, as discussed in the Introduction. Thereby, synchronization is likely due to a mixture of the various processes. However, hydrodynamic interactions clearly play a prominent role.

#### ACKNOWLEDGMENTS

We thank Shang-Yik Reigh for helpful discussions. Financial support by the VW Foundation (VolkswagenStiftung) within the program *Computer Simulation of Molecular and Cellular Bio-Systems as well as Complex Soft Matter* is gratefully acknowledged.

- 
- [1] A. Pikovsky, M. Rosenblum, and J. Kurths, *Synchronization: A Universal Concept in Nonlinear Science* (Cambridge University Press, Cambridge, UK, 2002).
  - [2] S. Strogatz, *Sync: How Order Emerges From Chaos in the Universe, Nature, and Daily Life* (Hyperion, New York, 2004).
  - [3] E. Lauga and T. R. Powers, *Rep. Prog. Phys.* **72**, 096601 (2009).
  - [4] G. Taylor, *Proc. R. Soc. London, Ser. A* **209**, 447 (1951).
  - [5] M. J. Kim and T. R. Powers, *Phys. Rev. E* **69**, 061910 (2004).
  - [6] M. Reichert and H. Stark, *Eur. Phys. J. E* **17**, 493 (2005).
  - [7] Y. W. Kim and R. R. Netz, *Phys. Rev. Lett.* **96**, 158101 (2006).
  - [8] P. Lenz and A. Ryskin, *Phys. Biol.* **3**, 285 (2006).
  - [9] A. Vilfan and F. Jülicher, *Phys. Rev. Lett.* **96**, 058102 (2006).
  - [10] C. M. Pooley, G. P. Alexander, and J. M. Yeomans, *Phys. Rev. Lett.* **99**, 228103 (2007).
  - [11] G. J. Elfring and E. Lauga, *Phys. Rev. Lett.* **103**, 088101 (2009).
  - [12] N. Uchida and R. Golestanian, *Phys. Rev. Lett.* **104**, 178103 (2010).
  - [13] N. Uchida and R. Golestanian, *Phys. Rev. Lett.* **106**, 058104 (2011).
  - [14] R. Golestanian, J. M. Yeomans, and N. Uchida, *Soft Matter* **7**, 3074 (2011).
  - [15] M. Leoni and T. B. Liverpool, *Phys. Rev. E* **85**, 040901(R) (2012).
  - [16] I. H. Riedel, K. Kruse, and J. Howard, *Science* **309**, 300 (2005).
  - [17] B. Qian, H. Jiang, D. A. Gagnon, K. S. Breuer, and T. R. Powers, *Phys. Rev. E* **80**, 061919 (2009).
  - [18] M. Polin, I. Tuval, K. Drescher, J. P. Gollub, and R. E. Goldstein, *Science* **325**, 487 (2009).
  - [19] R. E. Goldstein, M. Polin, and I. Tuval, *Phys. Rev. Lett.* **103**, 168103 (2009).
  - [20] J. Kotar, M. Leoni, B. Bassetti, M. C. Lagomarsino, and P. Cicuta, *Proc. Natl. Acad. Sci. USA* **107**, 7669 (2010).
  - [21] R. Di Leonardo, A. Búzás, L. Kelemen, G. Vizsnyiczai, L. Oroszi, and P. Ormos, *Phys. Rev. Lett.* **109**, 034104 (2012).
  - [22] J. K. G. Dhont, *An Introduction to Dynamics of Colloids* (Elsevier, Amsterdam, 1996).
  - [23] T. Niedermayer, B. Eckhardt, and P. Lenz, *Chaos* **18**, 037128 (2008).
  - [24] S. Y. Reigh, R. G. Winkler, and G. Gompper, *Soft Matter* **8**, 4363 (2012).
  - [25] S. Y. Reigh, R. G. Winkler, and G. Gompper (unpublished).
  - [26] B. M. Friedrich and F. Jülicher, *Phys. Rev. Lett.* **109**, 138102 (2012).
  - [27] R. R. Bennett and R. Golestanian, *Phys. Rev. Lett.* **110**, 148102 (2013).
  - [28] B. Eckhardt and E. Hascoët, *Phys. Rev. E* **72**, 037301 (2005).
  - [29] H. C. Berg, *E. coli in Motion* (Springer, New York, 2004).
  - [30] P. Espanol and P. B. Warren, *Europhys. Lett.* **30**, 191 (1995).
  - [31] C.-C. Huang, G. Gompper, and R. G. Winkler, *Phys. Rev. E* **86**, 056711 (2012).
  - [32] C.-C. Huang, G. Gompper, and R. G. Winkler, *J. Chem. Phys.* **138**, 144902 (2013).
  - [33] C. Lubich, *Numer. Math.* **40**, 119 (1982).
  - [34] N. Uchida and R. Golestanian, *Eur. Phys. J. E* **35**, 1 (2012).
  - [35] Y. Kuramoto, in *International Symposium on Mathematical Problems in Theoretical Physics*, edited by H. Arakai, Lecture Notes in Physics Vol. 39 (Springer, New York, 1975), p. 420.
  - [36] S. H. Strogatz, *Physica D* **143**, 1 (2000).
  - [37] L. Turner, W. S. Ryu, and H. C. Berg, *J. Bacteriol.* **182**, 2793 (2000).
  - [38] A. Malevanets and R. Kapral, *J. Chem. Phys.* **110**, 8605 (1999).
  - [39] R. Kapral, *Adv. Chem. Phys.* **140**, 89 (2008).
  - [40] G. Gompper, T. Ihle, D. M. Kroll, and R. G. Winkler, *Adv. Polym. Sci.* **221**, 1 (2009).